OPEN

PRS GLOBAL OPEN

ORIGINAL ARTICLE

Pediatric/Craniofacial

Classification of Subtypes of Apert Syndrome, Based on the Type of Vault Suture Synostosis

Xiaona Lu, MD*
Rajendra Sawh-Martinez, MD, MHS†
Antonio Jorge Forte, MD‡
Robin Wu, BS†
Raysa Cabrejo, BS†
Alexander Wilson, BS†
Derek M. Steinbacher, MD, DMD†
Michael Alperovich, MD†
Nivaldo Alonso, MD, PhD†§
John A. Persing, MD†

Background: Apert syndrome patients are different in clinical pathology, including obstructive sleep apnea, cleft palate, and mental deficiency. These functional deficiencies may be due to anatomic deformities, which may be caused by different forms of associated suture fusion. Therefore, a classification system of Apert syndrome based on the type of craniosynostosis pattern might be helpful in determining treatment choices.

Methods: CT scans of 31 unoperated Apert syndrome and 51 controls were included and subgrouped as: class I. Bilateral coronal synostosis; class II. Pansynostosis; and class III. Perpendicular combination synostosis: a. unilateral coronal and metopic synostosis; b. sagittal with bilateral/unilateral lambdoid synostosis; and c. others.

Results: Class I is the most common (55%) subtype. The cranial base angulation of class I was normal; however, the cranial base angulation on the cranium side of the skull in class II increased 12.16 degrees (P = 0.006), whereas the facial side cranial base angle of class IIIa decreased 4.31 degrees (P = 0.035) over time. The external cranial base linear measurements of class I showed more evident reduction in anterior craniofacial structures than posterior, whereas other subtypes developed more severe shortening in the posterior aspects.

Conclusions: Bicoronal synostosis is the most common subtype of Apert syndrome with the normalized cranial base angulation. Combined pansynostosis patients have flatter cranial base, whereas the combined unilateral coronal synostosis have a kyphotic cranial base. Class I has more significant nasopharyngeal airway compromise in a vertical direction, whereas classes II and III have more limited oropharyngeal space. *(Plast Reconstr Surg Glob Open 2019;7:e2158; doi: 10.1097/GOX.0000000000002158; Published online 20 March 2019.)*

INTRODUCTION

Despite the similar phenotypic characteristics of craniofacial malformations and syndactylism,[1,2] 81% of patients with Apert syndrome have obstructive sleep apnea, 76%–30% have cleft soft palate or bifid uvula, 70% have vertebral fusions, 48% have mental deficiency, 24% have cleft hard palate, and 10% have cardiovascular defects.[3–10] The variations of incidence of these morphological and functional defects in Apert syndrome cause questions: what is the primary reason of the high degree of variable phenotypical expressions? If there are subtypes in Apert, which are particularly related to specific morphologies?

Multiple patterns of premature fusion of cranial vault sutures exist in Apert syndrome, with the most common bilateral coronal synostosis.[11] Apert cranial base angulation is inconsistent as well. It was described as more obtuse than normal in studies of Kreiborg et al.[12] and Kitano

*From the *Plastic Surgery Hospital, Chinese Academy of Medical Sciences, Peking Union Medical College, Plastic Surgery Hospital, Beijing, China; †Section of Plastic and Reconstructive Surgery, Department of Surgery, Yale School of Medicine, New Haven, Conn.;‡Division of Plastic and Reconstructive Surgery, Mayo Clinic Florida, Jacksonville, Fla.; and §Department of Plastic Surgery, University of São Paulo, São Paulo, Brazil.*

Received for publication October 12, 2018; accepted December 5, 2018.

DOI: 10.1097/GOX.0000000000002158

Disclosure: *The authors have no financial interest to declare in relation to the content of this article.*

Supplemental digital content is available for this article. Clickable URL citations appear in the text.

et al.,[13] but also normal dimensions are discribed.[14] The (protentional) relationship among cranial vault sutures, cranial base, and facial characteristics have been recognized, and the cranial vault suture is the probable anatomic locus of disturbed growth.[14,15] Therefore, in this study, from the point of vault suture synostosis, Apert syndrome was classified into 3 subtypes, to explore the similarities and differences among them, to propose more individualized management plans.

PATIENTS AND METHODS

This study was approved by the Yale Human Investigation Committee (HIC 1101007932). Computed tomographic scans were obtained from all subjects without any previous surgical intervention. Unoperated Apert syndrome patients and age- and gender-matched controls were included. All the CT scans are divided into 3 types based on fully premature closure of sutures: class I. Bilateral coronal synostosis; class II. Pansynostosis; and class III. Perpendicular combination synostosis: a. unilateral coronal and metopic synostosis; b. sagittal with bilateral/unilateral lambdoid synostosis; and c. others.

Digital imaging was measured using Materialise software (version 19.0; Materialise, Leuven, Belgium). The Pearson correlation coefficients of interobserver (compared with practiced observers R.S. and A.F.) and intraobserver were >0.95. All the landmark points, generated lines and angles were measured twice by the same observer. The definitions of measurements were summarized (see table, **Supplemental Digital Content 1**, which displays the definition of landmarks, http://links.lww.com/PRSGO/B25; see table, **Supplemental Digital Content 2**, which displays the definition of cephalometric distances, angles, ratios, and planes, http://links.lww.com/PRSGO/B26). The comparisons were produced between each subtype and controls. The controls were reused and rematched for each subgroup. The Wilcoxon signed-rank test was performed using IBM SPSS Statistics 24 (IBM Corp., Armonk, N.Y.).

RESULTS

Thirty-one unoperated Apert syndrome patients and 51 age- and gender-matched controls were classified as 3 subgroups. The class I. Bilateral coronal synostosis, n = 17; class II. Pansynostosis, n = 6; and class III. Perpendicular combination synostosis: a. unilateral coronal and metopic synostosis, n = 3; b. sagittal with bilateral/unilateral lambdoidal, n = 3; and c. others, n = 2 (Fig. 1; Tables 1–2).

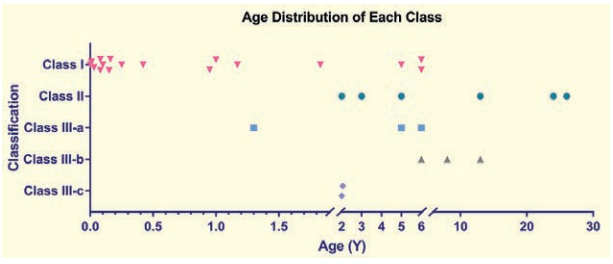

Fig. 1. Age distribution of each class in Apert syndrome.

CLASS I. BILATERAL CORONAL SYNOSTOSIS

Cranial Base

The entire cranial base length, from nasion (N) to basion (BA) reduced 12% ($P = 0.012$), with more evident shortened anteroposterior lengths related to middle cranial base (Fig. 2; Table 3). The distance from N to the sella (S) and ethmoid-sphenoid (ES) reduced 13% ($P = 0.012$) and 11% ($P = 0.022$), respectively. The distance S-BA, S to sphenooccipital synchondrosis (S-SO), and S-ES decreased 13% ($P = 0.005$), 20% ($P = 0.005$), and 14% ($P = 0.028$),

Table 1. Apert Syndrome Classification and Incidence of Each Type

Type	Synostosis Characteristics	Percentage (%)
Type I	Bilateral coronal synostosis	55
Type II	Pansynostosis	19
Type III	Perpendicular combination of synostosis	10
	a. Unilateral coronal + metopic synostosis	10
	b. Sagittal + bilateral/unilateral coronal synostosis	6
	c. Others	
Total		100

Table 2. Demographic Information of Apert and Controls

Group	Apert	Control	*P*
Type I			
Number	17	33	
Age (y)	1.37	1.40	0.95
AVE	2.12	1.89	
SD			
Gender			
Male	9	18	
Female	8	15	
Type II			
Number	6	12	
Age (y)	12.17	12.31	0.98
AVE	10.68	10.40	
SD			
Gender			
Male	1	5	
Female	5	7	
Type IIIa			
Number	3	15	
Age (y)	4.10	3.48	0.72
AVE	2.48	1.89	
SD			
Gender			
Male	3	9	
Female	0	6	
Type IIIb			
Number	3	16	
Age (y)	9.00	9.11	0.97
AVE	3.61	3.17	
SD			
Gender			
Male	3	9	
Female	0	7	
Type IIIc			
Number	2	4	
Age (y)	2.03	1.94	
AVE	0.04	0.41	
SD			0.70
Gender			
Male	0	2	
Female	2	2	

AVE, average; ACF, anterior cranial fossa width.

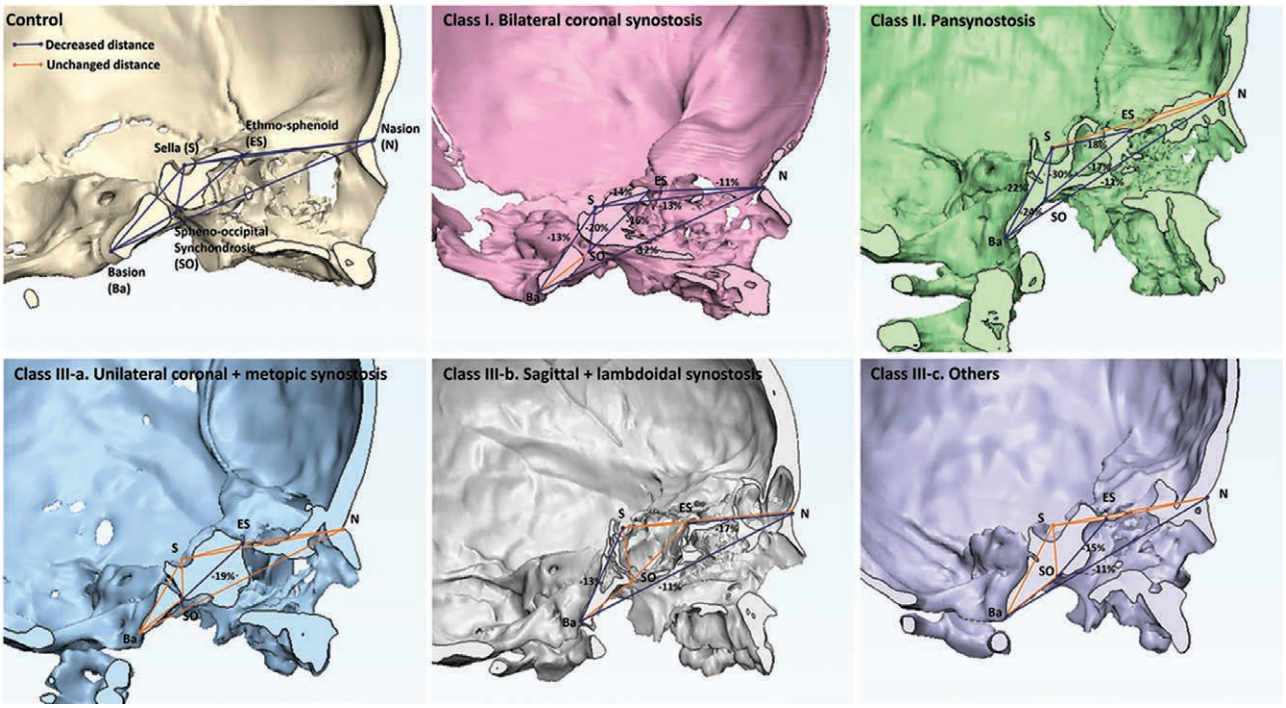

Fig. 2. Cranial base inner distances represented on sagittal view show the different changes in each subtype of Apert syndrome. Class I developed more evident shortened anteroposterior length of middle cranial base. Class II has a significantly shortened posterior cranial base. Three subtypes of class III developed inconsistently decreased cranial base length.

respectively. The cranial base angulation, however, is normal (Fig. 3).

The external cranial base linear measurements showed more evident reduction in the in anterior craniofacial structures than posterior (Fig. 4). The distance between posterior nasal spine (PNS) to N, ES, and S reduced 23% ($P = 0.001$), 23% ($P = 0.001$), and 16% ($P = 0.039$), whereas the distance PNS-Ba grew parallel to normal.

Craniofacial Relationships

The angle from SN plane and Frankfort horizontal (FH) plane to Maxillary (Mx) plane significantly increased 9.11 degrees ($P < 0.001$) and 7.44 degrees ($P = 0.008$), respectively. The angle between Mx and the occlusal (Occ) planes decreased 7.99 degrees ($P = 0.004$), accompanied by slightly increased plane angles (see figure, **Supplemental Digital Content 3**, which displays the 6 facial anatomic planes were used in this study. The angles among these planes were measured for analyzingthe craniofacial relationship differences among the 4 classes of Apert syndrome. Apert class I was used as reference, http://links.lww.com/PRSGO/B27).

The linear measurements, with the S as the reference point showed limited anteroposterior development of entire facial structures. The distance S-ANS, S-A, and S-B decreased by 20% ($P < 0.001$), 20% ($P < 0.001$), and 19% ($P = 0.003$), respectively. The distances of S-Pogonion (Pog), S-Gnathion (GN), S-Gonion (GO), and S-Articulare decreased by 20% ($P = 0.003$), 21% ($P = 0.003$), 15% ($P = 0.044$), and 12% ($P = 0.010$), respectively, suggesting the anterior facial structures developed more evident length compromise than posterior facial structures.

Orbit

The orbit length was reduced by 19% ($P < 0.001$), but with normalized orbit height, width, and outside horizontal angle. The occupancy of ethmoid side angle and sphenoid side angle of the outside horizontal angle was greater, 17% ($P < 0.001$) and 8% ($P = 0.002$). Consequently, the inside horizontal angle was smaller 31% ($P < 0.001$) (Fig. 5 and see figure, **Supplemental Digital Content 4**, which displays the orbit horizontal angles illustrated in each category, http://links.lww.com/PRSGO/B28). The vertical angle increased 7.11 degrees ($P < 0.001$). The globe protrusion increased 127% ($P < 0.001$).

The relationship between the orbits bilaterally, the ethmoid roll angle increased by 10.39 degrees ($P < 0.001$), and the distance between bilateral ethmoid midpoints increased 27% ($P = 0.002$). Consequently, the angle between bilateral optical axes was greater than 8.40 degrees ($P < 0.001$).

Midface

The zygomatic anterior protrusion reduced 19% ($P < 0.001$), with increased zygoma transverse width (33%, $P < 0.001$). The angle among S and zygoma peak points (ZPR-S-ZPL) increased 21 degrees ($P < 0.001$); however, the distance between the bilateral zygoma peak points (ZPR-ZPL) was reduced 15.04 ml ($P < 0.001$). The distance ANS-PNS reduced 32% ($P < 0.001$), and the distance between ASN and medial pterygoid plate (ASN-PP), indicating the anteroposterior Mx length, decreased 25% ($P < 0.001$). The nasal base width narrowed 20% ($P = 0.001$) as well. In the vertical direction, the distance Rhinion-ANS reduced 20% ($P = 0.013$). The above results illustrated the midface aplasia developed in all anteroposterior, mediolateral, and vertical directions.

Table 3. The Measurement Results with Statistical Significance of Class I (Bilateral Coronal Synostosis)

	Class I				
	Bicoronal		Control		Rank Test
Index	AVE	SD	AVE	SD	*P*
Cranial base					
ACF	19.97	6.29	11.58	2.71	<0.001††
N-BA	64.73	10.99	73.58	10.49	0.012*
N-S	43.16	7.81	49.37	7.54	0.012*
N-ES	28.62	4.36	32.17	4.79	0.022*
S-BA	26.79	3.99	30.89	4.47	0.005†
S-SO	12.71	3.43	15.98	3.58	0.005†
SO-ES	22.55	4.99	26.80	5.31	0.010†
S-ES	15.16	3.80	17.61	4.01	0.028*
Sphenoid greater wing angle	108.98	10.84	95.81	10.34	0.001†
N-PNS	34.35	9.84	44.45	8.42	0.001†
ES-PNS	20.91	5.93	27.16	5.44	0.001†
S-PNS	24.94	5.50	29.59	6.11	0.039*
S-ANS	46.31	8.41	57.86	9.01	<0.001†
BA-ANS	57.32	9.75	70.34	8.88	<0.001†
S-ARR/L	35.72	6.92	40.68	5.23	0.010*
Craniofacial relationship					
SN/Mx	14.71	5.89	5.61	4.28	<0.001†
FH-Mx	8.18	10.84	0.74	4.44	0.008†
Mx/Occ	0.99	8.37	8.97	6.25	0.004†
SNA	77.90	9.21	85.98	3.86	0.002†
ANB	0.11	8.74	5.49	3.68	0.025*
N-S-GN	66.79	11.43	58.63	4.92	0.032*
S-A	46.13	8.24	57.40	9.03	<0.001†
S-B	55.88	14.18	69.20	13.70	0.003†
S-Pog	59.09	14.95	73.99	15.24	0.003†
S-GN	59.75	15.73	75.60	15.69	0.003†
S-PNS	24.94	5.49	29.59	6.11	0.040*
S-GO	47.10	12.90	55.18	10.88	0.044*
ANS-S	46.32	8.41	57.86	9.01	<0.001†
ANS-BA	57.32	9.75	70.34	8.88	<0.001†
ANS-PNS	24.52	6.60	36.18	5.46	<0.001†
Orbit					
Orbit length	29.61	4.63	36.70	5.54	<0.001†
Vertical cone angle	61.91	7.67	54.80	4.06	<0.001†
GPR/L	10.97	3.10	4.83	1.51	<0.001†
Visual axis length/orbital length	1.30	0.11	1.06	0.06	<0.001†
OrL-OrR	57.39	11.15	48.46	5.33	0.002†
Bilateral optical axis angle	51.28	5.86	42.88	5.51	<0.001†
Roll angle of ethmoid	5.98	3.88	−4.42	4.46	<0.001†
Ethmoid middle width	21.47	6.22	16.90	3.52	0.002†
Inside horizontal angle%	0.75	0.19	1.06	0.08	<0.001†
Ethmoid side angle%	0.14	0.11	−0.04	0.07	<0.001†
Sphenoid side angle%	0.09	0.13	0.02	0.06	0.002†
Midface					
Zygomatic protrusion	34.53	6.37	42.85	6.81	<0.001†
ZPR-S-ZPL	90.94	5.66	69.91	7.71	<0.001†
ZPR-ZPL	69.68	13.20	84.72	6.09	<0.001†
Zygoma transverse width	7.43	1.19	5.57	1.15	<0.001†
Zygoma length	28.60	7.35	35.36	5.45	0.001†
Bizygomatic width	75.46	16.23	85.04	12.09	0.021*
ANS-PP	33.23	7.26	44.19	5.99	<0.001†
NcR-NcL	15.90	4.02	19.95	2.82	0.001†
Rhinion-ANS	15.36	3.79	19.16	7.90	0.013*
Mandible					
COR-COL	56.48	11.40	67.63	9.28	0.002†
GOR-GOL	51.20	11.54	62.47	9.02	0.001†
COR/L-GOR/L	22.99	10.33	31.39	10.75	0.004†
GOR/L-Pog	42.35	8.79	54.08	9.24	<0.001†
COR/L-Pog	56.26	13.32	75.25	13.85	<0.001†
CO-GO/GO-Pog	0.49	0.09	0.59	0.16	0.013*
COR/L-A	51.17	9.88	68.37	9.86	<0.001†

*P < 0.05.
†*P* < 0.01. AVE, average; ACF, anterior cranial fossa width.

Mandible

The mandibular linear measurements of Apert syndrome patients in this subtype presented holistic shortening. The distance between bilateral condylions (COR-COL) and the distance between bilateral GO (GOR-GOL) decreased 16% (*P* = 0.002) and 18% (*P* = 0.001), respectively. The mandible ramus height (COR/L-GOR/L) reduced 27% (*P* = 0.004). The mandibular body length (GOR/L-Pog) and mandibular length (COR/L-Pog) decreased 22% and 25% (both *P* < 0.001). The mandibular angulations are normal.

CLASS II. PANSYNOSTOSIS

Cranial Base

The entire cranial base length and the anterior cranial base length grew almost normally (insignificantly shorter than normal). The distances S-BA, S-SO, and S-ES reduced 22% (*P* = 0.013), 30% (*P* = 0.002), and 18% (*P* = 0.032), respectively. The cranial base angulation in cranium side (N-S-BA) increased 12.16 degrees (*P* = 0.001), indicating a more flat cranial base. The decreased distances of BA-PNS (24%, *P* = 0.003), S-PNS (29%, *P* = 0.007), S-ANS (20%, *P* = 0.003), and BA-ANS (17%, *P* = 0.013) suggested a reduced volume of the entire upper airway (Table 4).

Craniofacial Relationship

The SN-FH angle increased 8.21 degrees (*P* = 0.001), the SN-Mx angle increased 8.06 degrees (*P* = 0.003), and the SN-MP and SN-MRP angles significantly increased 19.32 degrees (*P* < 0.001) and 12.97 degrees (*P* = 0.002), respectively. Relative to the FH plane, the Occ plane was rotated anticlockwise by 5.87 degrees (*P* = 0.041). The angles N-S-PP, N-A-Pog, and N-S-GN increased 8.79 degrees (*P* = 0.003), 19.74 degrees (*P* < 0.001), and 13.86 degrees (*P* < 0.001), respectively. The angle S-N-Pog decreased 9.28 degrees (*P* = 0.027). These changed angles and reduced distances indicating the holistic shortening of facial structures anteroposteriorly and developed a posterior and inferior rotation, relative to the cranial base.

Facial Feature

The orbit length reduced 26% (*P* < 0.001), whereas the orbit height increased 16% (*P* = 0.001), with the normalized orbit width, but a less inside horizontal angle (24%, *P* = 0.001). The relative position of bilateral orbits developed wider. The angle between bilateral optical axes was greater by 13.05 degrees (*P* = 0.024) when compared with controls. The zygomatic anterior prominence was reduced 20.92 mm (*P* < 0.001), with reduced Mx anteroposterior length (*P* = 0.018), but the mediolateral width of midface was within the normal range. The mandible had a similar size versus controls.

CLASS III. PERPENDICULAR COMBINATION OF SYNOSTOSIS

Class IIIa. Unilateral Coronal with Metopic Synostosis

Cranial Base

Apert syndrome patients in this group did not have statistically significant widened anterior cranial fossa

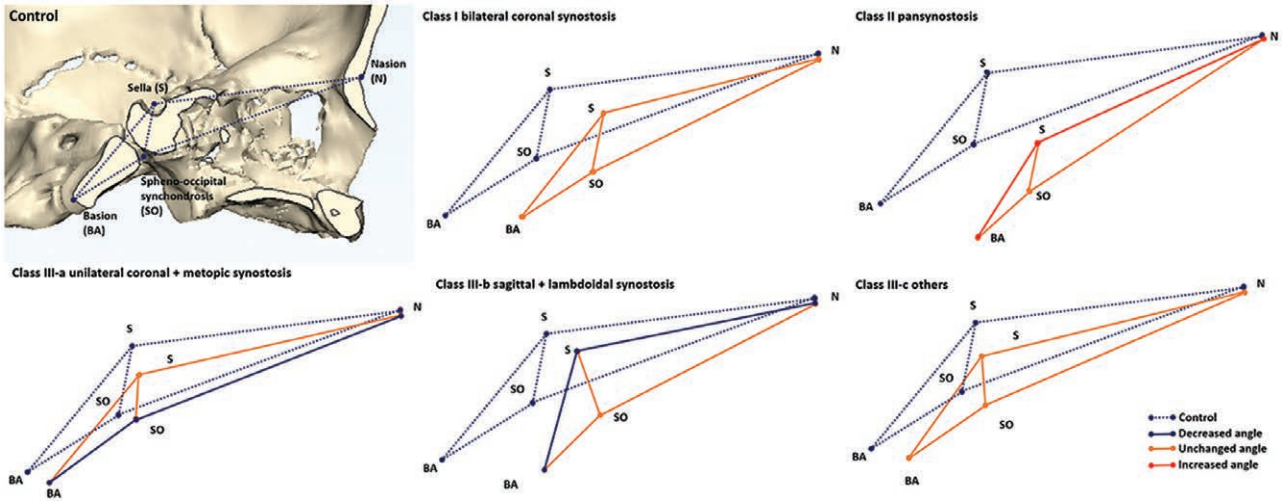

Fig. 3. The geometric graphs show the changes of cranial base angulations. Class II had more obtuse cranial base angulation in cranium side (N-S-BA), with a thinner cranial base. Class IIIa had narrower N-SO-BA angle, indicating the kyphotic cranial base on the "facial side," of this subtype. Class IIIb had narrower N-S-BA, with a thicker cranial base. The cranial base angles of classes I and IIIc grew parallel to normal. Dotted lines represented controls, and the bold lines represent Apert syndrome.

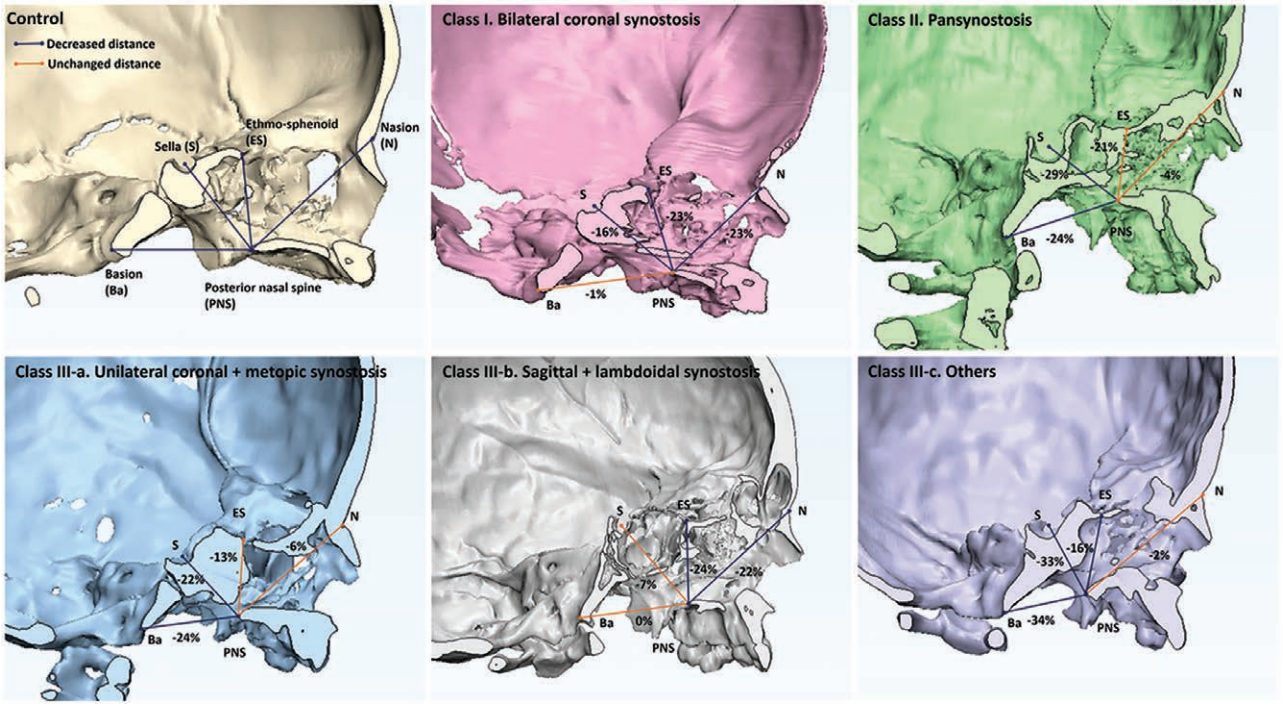

Fig. 4. The external cranial base linear measurements show classes I and IIIb have more evident reduction distances in anterior craniofacial structures than posterior, suggesting linkage to the more limited nasal and nasopharyngeal airway space. The entire upper airway of class II is compromised. Class IIIa has more limited oropharyngeal space. The numbers marked in figures are the percentage changes of each subgroup compared with controls.

or shortened overall cranial base length. They developed shortened anteroposterior length of the sphenoid (P = 0.002). The angles N-S-SO were less 11.29 degrees (P = 0.017) (see figure, **Supplemental Digital Content 5**, which displays the complete set of all measurement results of all categories, http://links.lww.com/PRSGO/B29). The shortened distances BA-PNS (24%, P = 0.002) and S-PNS (22%, P = 0.002) suggested the significantly reduced volume of pharyngeal airway. The distance of ANS-Ba reduced 18% (P = 0.002), indicating a shortened midfacial anteroposterior length.

Craniofacial Features

Relative to the SN plane, the Mx plane and mandibular plane rotated clockwise 9.84 degrees (P = 0.002) and 16.62 degrees (P = 0.005), respectively. The angle FH-Mx

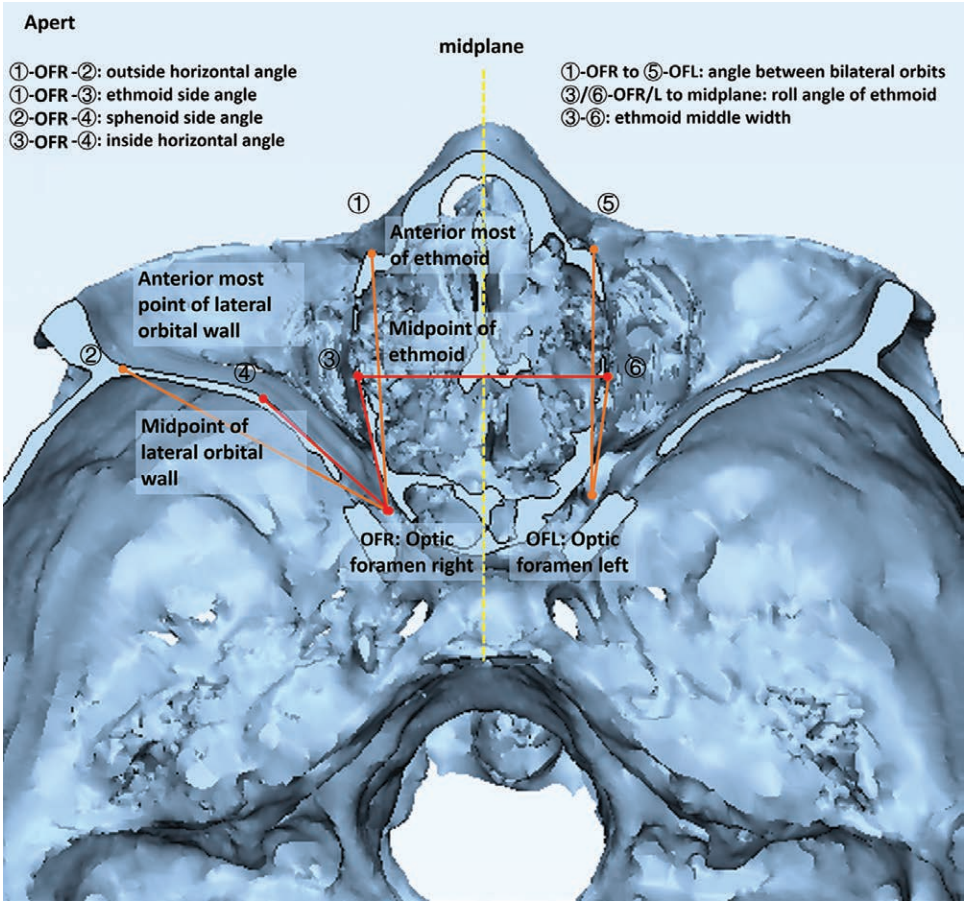

Fig. 5. Orbital special measurements are illustrated.

made the most contribution by 8.74 degrees ($P = 0.002$). The angles SNA and ANB reduced 11.11 and 6.31 degrees (both $P = 0.02$). The angle N-S-GN widened 12.77 degrees ($P = 0.005$), whereas the angle S-N-Pog narrowed 7.26 degrees ($P = 0.005$). Orbital and midfacial features of this group Apert were similar to class I, except for the normalized mandible and increased Mx width (ZMR-ZML) (22%, $P = 0.010$).

Class IIIb. Sagittal and Bilateral/Unilateral Lambdoidal Synostosis

Cranial Base

The anterior cranial fossa width is increased 79% ($P = 0.005$), with the shortened, entire, cranial base length (11%, $P = 0.005$). The cranial base angulation in cranium side (N-S-BA) reduced 10.78 degrees ($P = 0.005$), whereas the angle in facial side is parallel to controls (Fig. 3). The external linear measurements showed the more evident limited subcranial distance anteriorly than posteriorly. The distance between N-PNS and ES-PNS reduced 22% ($P = 0.005$) and 24% ($P = 0.022$). Both distances from ANS to S and BA were reduced, by 17% and 22% (both $P = 0.005$).

Craniofacial Features

The planar angle FH-Occ increased 7.23 degrees ($P = 0.005$), indicating a clockwise-rotated Occ plane, which is different from other subgroups. The angles SNA and ANB reduced 15.15 and 12.03 degrees (both $P = 0.005$), with the normalized SNB. The point A was retreated 11.50 mm (P=0.011), based on Wit's measurements. These findings are consistent with the significant retrusive midface structures. Other facial features were similar to class II.

Class IIIc. Others

Apert patients in this subgroup have bilateral coronal and bilateral lambdoidal synostosis with/without metopic synostosis at the same time. Because of a lesser frequency and disparate pathologies, no statistical comparison could be made accurately. Findings, however, are presented for completeness.

The sphenoid greater wing angle was normalized, but the separation of lateral PPs was increased by 8.41 degrees. The distances from PNS to ES, S, and BA reduced 16%, 33%, and 34%, respectively. Both distances from ANS to S and BA was reduced by 23%. The occlusive plane was rotated anticlockwise, represented by the reduced FH-OCC plane angle (15.34 degrees), and resulted in the reduced Mx-Occ angle (13.02 degrees) and increased Occ-MP angle (19.14 degrees). The angles of SNA and ANB were reduced 18.82 and 20.82 degrees, respectively. The point A was retro positioned by 12.78 mm, based on Wit's measure-

Table 4. The Measurement Results with Statistical Significance of Class II (Pansynostosis)

	Class II				
	Pansynostosis		Control		Rank Test
Index	AVE	SD	AVE	SD	*P*
Cranial base					
ACF	26.72	4.31	16.91	4.30	<0.001†
S-BA	31.65	4.54	40.63	5.93	0.013*
S-SO	15.47	1.81	22.00	5.08	0.002†
SO-BA	17.31	2.10	22.92	3.34	0.001†
SO-ES	28.76	3.53	34.83	6.37	0.083
S-ES	18.57	1.93	22.59	4.57	0.032*
Sphenoid greater wing angle	118.04	7.58	89.79	6.22	<0.001†
N-S-BA	140.87	6.99	128.72	4.63	0.001†
BA-S-ES	139.03	9.39	127.76	6.84	0.024*
BA-PNS	31.18	5.83	40.92	4.66	0.003†
S-PNS	29.33	5.94	41.58	8.21	0.007†
S-ANS	59.95	6.96	75.28	11.44	0.003†
BA-ANS	72.57	9.07	87.89	11.30	0.013*
Craniofacial relationship					
SN/FH	16.22	3.87	8.01	3.90	0.001†
SN/Mx	14.81	7.06	6.75	3.10	0.003*
SN/MP	53.66	3.77	34.34	4.93	<0.001†
SN/MRP	98.76	3.55	85.79	8.15	0.002†
FH/Occ	4.16	5.17	10.03	5.48	0.041*
FH/MP	36.25	4.77	27.52	5.43	0.006†
Occ/MP	33.37	4.21	16.32	3.23	<0.001†
SNA	67.00	4.24	84.86	5.41	<0.001†
SNB	72.98	4.23	80.98	7.30	0.019*
N-S-PP	86.96	5.58	78.17	3.48	0.003†
N-A-Pog	191.98	6.27	172.24	6.77	<0.001†
N-S-GN	78.21	2.05	64.35	5.25	<0.001†
S-N-Pog	71.65	4.84	80.92	7.28	0.027*
S-A	57.45	7.35	74.96	11.98	0.003†
S-PNS	29.33	5.94	41.58	8.21	0.007†
ANS-S	59.95	6.95	75.28	11.44	0.003†
ANS-BA	72.56	9.05	87.89	11.29	0.013*
Wit's	-8.60	5.72	3.24	3.31	<0.001†
Orbit					
Orbit length	34.28	4.06	46.26	5.18	<0.001†
Orbit height	38.36	2.37	33.07	2.75	<0.001†
Orbital rim angle	108.10	6.72	118.59	4.40	0.003†
GPR/L	13.92	2.43	5.70	2.11	<0.001†
Visual axis length/orbital length	1.39	0.12	1.03	0.04	<0.001†
UORL-UORR	65.72	7.09	52.08	6.95	0.007†
Cornea r-cornea l	70.73	7.99	58.42	7.67	0.007*
Bilateral optical axis angle	52.63	9.18	39.58	2.02	0.024*
Outside horizontal angle	67.62	3.53	56.97	3.43	<0.001†
Ethmoid middle width	30.24	4.28	24.88	4.66	0.053
Inside horizontal angle%	0.76	0.11	1.00	0.07	0.001†
Ethmoid side angle%	0.16	0.05	0.06	0.07	0.010*
Midface					
Zygomatic protrusion	42.44	3.72	63.36	23.54	<0.001†
ZPR-S-ZPL	96.18	5.50	84.81	9.52	0.013*
Zygoma length	38.41	3.66	44.84	6.41	0.024*
ANS-PP	46.85	5.44	55.77	7.31	0.018*
Mandible					
ARR/L-GOR/L-N	52.02	5.69	60.74	7.08	0.037*
N-GOR/L-Men	78.20	1.61	65.78	2.73	<0.001†
COR/L-A	69.18	8.62	88.13	13.07	0.007†

*$P < 0.05$.

†$P < 0.01$. AVE, average; ACF, anterior cranial fossa width.

ments. These findings are consistent with the significant retrusive midface structures. Apert syndrome patients in this group developed higher orbit height with normal orbit length and width, which is different with the other 3 groups. The orbital rim angle was narrower by 14.27 degrees. The globe protrusion was increased by 247%, which is the most severe, and resulted in a bigger ratio of visual axis length to orbital length (33%). The distance of MOR-MOL, UORR-UORL, and OrL-OrR showed almost proportionate increase. The maxilla was anteroposteriorly shortened by 20% and was mediolaterally narrowed when measured by bilateral J points (15%). Correspondingly, the nasal base width (NcR-NcL) decreased 12%.

DISCUSSION

Bilateral coronal synostosis is the most common subtype in Apert syndrome.[11] Other combinations include unilateral coronal synostosis, metopic or lambdoid synostosis, and interdigitation of them, but combined with sagittal synostosis is rare.[11,16] Interaction effects among vault sutures, cranial base, and facial features, the premature fused vault sutures may make more contributions to the malformed craniofacial features,[14,15] compromised respiratory, and visual impairment of Apert syndrome.[17,18] Therefore, fully premature fusion of these sutures was used as the criterion for classification in this study.

In this study, Apert syndrome developed classic brachycephaly, increased anterior cranial fossa width, accompanying with the increased sphenoid greater wing angle, and most evident a shortened cranial base length.[3] Overall, the cranial base angulation of most Apert patitents in the sagittal plane is normal, except for a slightly flatter cranial base angle in class II and kyphotic cranial base in class IIIa, which explains the inconsistent results of cranial base angulation measurements of Apert syndrome in past studies. Kreiborg et al.[12] and Kitano et al.[13] reported increased cranial base angle, but in the most, the cranial base angulation was documented as normal.[14] The cranial base angulation in sagittal plane of unilateral coronal synostosis in both syndromic and nonsyndromic craniosynostosis was not fully studied, except their deviations from midline.[19,20]

The external cranial base linear measurements illustrate variants among subtypes, although most of them were reduced, when compared with normal controls. The Apert class I has more evidently reduced distances from anterior and middle cranial base to the PNS, with a normal distance between BA and the PNS. This result indicates a more limited nasal and nasopharyngeal space, than oropharyngeal space, when bilateral coronal synostoses occur in Apert syndrome. However, in class II, from anterior to posterior, the degree of reduction in length between cranial landmarks and the PNS was more marked. This is associated with a significantly reduced distance between BA and the PNS, indicating a smaller oropharynx. Considering class I (bilateral coronal synostosis) accounts for 55% of all Apert subjects in this study; these findings explained the variability of airway compromise of Apert syndrome patients in previous reports: most of Apert children were tracheotomized in their early infancy, but only a small percentages in older patients.[21] After cleft palate repair, some patients have greater airway compromise because the additional nasopharyngeal airway provided by the open cleft was diminished.[21]

This diversity was supported by Calandrelli et al.,[22] who deemed the airway obstruction is more sensitive to the pattern of premature synostosis, rather than a certain cranio-

synostosis syndrome. Furthermore, for Apert class I, the surgical intervention including downward vertical movement of the midface, in addition to horizontal advancement, is expected to protect the respiratory function, whereas classes II and IIIa and IIIc need more anterior advancement, or tonsillectomy and adenoidectomy as adjunctive procedures.[23]

Meanwhile, the relative position, morphology, and structure of mandible may be another contributor to respiratory compromise.[24] In class I, the linear measurements with S as reference points, the distance from S to the middle and lower facial landmarks of class I patients, developed wide spread decreases. These proportionate reduced diameters of maxilla and mandible to the S indicate a mutual adaptation and displacement of them. The volume of maxilla and mandible was slightly smaller compared with unaffected individuals in all subtypes, but without significant statistical difference. This is as the same finding in the studies of Forte et al.[14] and Calandrelli et al.[22] The significantly reduced mandibular bicondylar distance and GO distance reflect restricted horizontal development of oropharyngeal width, suggesting for class I patients, the respiratory problems potentially are more acute in the nasal and nasopharyngeal levels (limited vertical dimension) and oropharyngeal levels (limited transverse dimensions), and vector specified interventions on them may be more effective in increasing airway patency.[25,26] Le Fort osteotomies advocated by Tessier[27] are based on horizontal movement rather than vertical. This may explain why the airway seems been enlarged after Le Fort I/III or monobloc advancement, but there is no significant relationship between advancement and airway volume changes, and no respiratory improvement.[28,29] Mandibular advancement seems to be needed to create more space at the level of hypopharynx, especially for classes II and IIIa and IIIc.[30]

Orbital malformation is another characteristic of Apert, and it is diverse among these subgroups. The shorten anteroposterior orbit length was developed in all subtypes, but the coronal synostosis subgroups (I and IIIa; Fig. 5; see figure, **Supplemental Digital Content 4**, which displays the orbit horizontal angles illustrated in each category, http://links.lww.com/PRSGO/B28) have more evidently increased orbit height and vertical cone angle. Meanwhile, they have significantly smaller inside horizonal angle than other subtypes, associated with the prominent anterior lateral orbital wall and expanded mediolateral medial orbital wall, related to misshaped sphenoid and ethmoid bones.[31–33]

The nonsyndromic coronal synostosis patients also developed brachycephaly and a shorter anterior cranial fossa, elevated sphenoid, and shallow orbit,[15,34] which is similar to Apert syndrome patients. But the most marked protrusion of the lateral orbital wall is evident in Apert classes I, II, and IIIa. It is postulated that the premature fusion of coronal sutures, which limited the anterior expansion of anterior cranial base, the orbital upper wall, and limited the anteroposterior growth of middle cranial base, the bent and backward rotated sphenoid, changes the direction of the middle cranial fossa, and results in a curved lateral orbital wall.[35,36] The lateral ballooning of ethmoid is also found in other forms of craniosynostosis,[37,38] but the exaggerated protrusion of the lateral orbital wall is documented only in Apert syndrome to our knowledge.[39–41] There is a reduced occupancy of the effective horizonal space (the inside horizonal angle, Fig. 5) in the bony orbit. In this situation, frontofacial bipartition distraction, as the combination of the advantages of facial bipartition (correcting hypertelorism) and the advantages of monobloc distraction (advancing the midface), could be helpful to correct the orbital malformation and the anteroposterior midface hypoplasia at the same time.[26,42] Furthermore, the comparison in bilateral coronal synostosis between syndromic and nonsyndromic craniosynostosis could be helpful to illustrate the individual effect of syndrome and coronal suture system on craniofacial, especially the orbital, development.

The limitation of this study is the relative small number of patients in classes II and III. The requirement for this study was no previous surgical intervention. As Apert syndrome is a relatively uncommon from of craniosynostosis (occurs in approximately 1 in 65,000–88,000 newborns)[43] and classes II and III have a lower frequency of occurrence compared with class I, we decided to present the current data anticipating that it would be unlikely significant numbers added to these two groups over many years. However, optimally, it would ideal to have CT scans at a single time point as this might have impacted subtype classification. It is unreliable to speculate on the natural progression of the sutures fusion in Apert syndrome patients, due to the surgical interventions. Therefore, a further longitudinal study is needed to clarify the duration of the classification of each patient. Second, we did not collect data of the real-time respiratory function assessments or sleep study of patients. However, conjoint analysis of respiratory function outcome and cephalometric measurement could reveal a correlation between function and structure malformation of this particular group of patients. The present dataset, however, is designed to fast define accurately, anatomic detail of the Apert craniofacial skeleton and densely relevant to provide useful information. In this study, our focus was to specifically address the anatomy details of each subtype to ultimately take into account the relative anatomy distortions of the airway construction, to any airway compromise. Finally, we do not have the access of the genetic information of all our Apert patients. However, the correlation between each subgroup and their genetic features is a study on which we are working.

CONCLUSIONS

Bicoronal synostosis is the most common subtype of Apert syndrome (class I) with a normalized cranial base angulation. However, the Apert syndrome combined pansynostosis (class II) has flatter cranial base, whereas the combined unilateral coronal synostosis is associated with a kyphotic cranial base. Class I has more significant nasopharyngeal airway compromise in the vertical direction, whereas classes II, IIIa, and IIIc have more limited oropharyngeal space. Meanwhile, the restricted horizontal

development of oropharynx caused by narrower mandible worsens the respiratory obstruction in class I.

John A. Persing, MD
Section of Plastic and Reconstructive Surgery
Yale School of Medicine
330 Cedar Street
3rd Floor Boardman Building
New Haven, CT 06520
E-mail: john.persing@yale.edu

REFERENCES

1. Kim H, Uppal V, Wallach R. Apert syndrome and fetal hydrocephaly. *Hum Genet.* 1986;73:93–95.
2. Kreiborg S, Cohen MM Jr. Characteristics of the infant Apert skull and its subsequent development. *J Craniofac Genet Dev Biol.* 1990;10:399–410.
3. Avantaggiato A, Carinci F, Curioni C. Apert's syndrome: cephalometric evaluation and considerations on pathogenesis. *J Craniofac Surg.* 1996;7:23–31.
4. Kreiborg S, Cohen MM Jr. The oral manifestations of Apert syndrome. *J Craniofac Genet Dev Biol.* 1992;12:41–48.
5. Cohen MM Jr, Kreiborg S. Visceral anomalies in the Apert syndrome. *Am J Med Genet.* 1993;45:758–760.
6. Inverso G, Brustowicz KA, Katz E, et al. The prevalence of obstructive sleep apnea in symptomatic patients with syndromic craniosynostosis. *Int J Oral Maxillofac Surg.* 2016;45:167–169.
7. Tan AP, Mankad K. Apert syndrome: magnetic resonance imaging (MRI) of associated intracranial anomalies. *Childs Nerv Syst.* 2018;34:205–216.
8. Arroyo Carrera I, Martínez-Frías ML, Marco Pérez JJ, et al. Apert syndrome: clinico-epidemiological analysis of a series of consecutive cases in Spain. *An Esp Pediatr.* 1999;51:667–672.
9. Batra P, Duggal R, Parkash H. Dentofacial characteristics in Apert syndrome: a case report. *J Indian Soc Pedod Prev Dent.* 2002;20:118–123.
10. Stavropoulos D, Tarnow P, Mohlin B, et al. Comparing patients with Apert and Crouzon syndromes–clinical features and craniomaxillofacial surgical reconstruction. *Swed Dent J.* 2012;36:25–34.
11. Cohen MM Jr, Kreiborg S. Suture formation, premature sutural fusion, and suture default zones in Apert syndrome. *Am J Med Genet.* 1996;62:339–344.
12. Kreiborg S, Marsh JL, Cohen MM Jr, et al. Comparative three-dimensional analysis of CT-scans of the calvaria and cranial base in Apert and Crouzon syndromes. *J Craniomaxillofac Surg.* 1993;21:181–188.
13. Kitano I, Park S, Kato K, et al. Craniofacial morphology of conotruncal anomaly face syndrome. *Cleft Palate Craniofac J.* 1997;34:425–429.
14. Forte AJ, Alonso N, Persing JA, et al. Analysis of midface retrusion in Crouzon and Apert syndromes. *Plast Reconstr Surg.* 2014;134:285–293.
15. Furuya Y, Edwards MS, Alpers CE, et al. Computerized tomography of cranial sutures. Part 2: abnormalities of sutures and skull deformity in craniosynostosis. *J Neurosurg.* 1984;61:59–70.
16. Kreiborg S, Prydsoe U, Dahl E, et al. Clinical conference I. Calvarium and cranial base in Apert's syndrome: an autopsy report. *Cleft Palate J.* 1976;13:296–303.
17. Driessen C, Joosten KF, Bannink N, et al. How does obstructive sleep apnoea evolve in syndromic craniosynostosis? A prospective cohort study. *Arch Dis Child.* 2013;98:538–543.
18. Tay T, Martin F, Rowe N, et al. Prevalence and causes of visual impairment in craniosynostotic syndromes. *Clin Exp Ophthalmol.* 2006;34:434–440.
19. Abramson DL, Janecka IP, Mulliken JB. Abnormalities of the cranial base in synostotic frontal plagiocephaly. *J Craniofac Surg.* 1996;7:426–428.
20. Marsh JL, Gado MH, Vannier MW, et al. Osseous anatomy of unilateral coronal synostosis. *Cleft Palate J.* 1986;23:87–100.
21. Sculerati N, Gottlieb MD, Zimbler MS, et al. Airway management in children with major craniofacial anomalies. *Laryngoscope.* 1998;108:1806–1812.
22. Calandrelli R, Pilato F, Massimi L, et al. Quantitative evaluation of facial hypoplasia and airway obstruction in infants with syndromic craniosynostosis: relationship with skull base and splanchnocranium sutural pattern. *Neuroradiology.* 2018;60:517–528.
23. Saltaji H, Altalibi M, Major MP, et al. Le Fort III distraction osteogenesis versus conventional Le Fort III osteotomy in correction of syndromic midfacial hypoplasia: a systematic review. *J Oral Maxillofac Surg.* 2014;72:959–972.
24. Shilo D, Emodi O, Aizenbud D, et al. Controlling the vector of distraction osteogenesis in the management of obstructive sleep apnea. *Ann Maxillofac Surg.* 2016;6:214–218.
25. Ko EWC, Chen PKT, Tai ICH, et al. Fronto-facial monobloc distraction in syndromic craniosynostosis. Three-dimensional evaluation of treatment outcome and facial growth. *Int J Oral Maxillofac Surg.* 2012;41:20–27.
26. Crombag GA, Verdoorn MH, Nikkhah D, et al. Assessing the corrective effects of facial bipartition distraction in Apert syndrome using geometric morphometrics. *J Plast Reconstr Aesthet Surg.* 2014;67:e151–e161.
27. Tessier P. Total osteotomy of the middle third of the face for faciostenosis or for sequelae of Le Fort 3 fractures. *Plast Reconstr Surg.* 1971;48:533–541.
28. Nout E, Bannink N, Koudstaal MJ, et al. Upper airway changes in syndromic craniosynostosis patients following midface or monobloc advancement: correlation between volume changes and respiratory outcome. *J Craniomaxillofac Surg.* 2012;40:209–214.
29. Nout E, Bouw FP, Veenland JF, et al. Three-dimensional airway changes after Le Fort III advancement in syndromic craniosynostosis patients. *Plast Reconstr Surg.* 2010;126:564–571.
30. Bannink N, Nout E, Wolvius EB, et al. Obstructive sleep apnea in children with syndromic craniosynostosis: long-term respiratory outcome of midface advancement. *Int J Oral Maxillofac Surg.* 2010;39:115–121.
31. Seeger JF, Gabrielsen TO. Premature closure of the frontosphenoidal suture in synostosis of the coronal suture. *Radiology.* 1971;101:631–635.
32. Burdi AR, Kusnetz AB, Venes JL, et al. The natural history and pathogenesis of the cranial coronal ring articulations: implications in understanding the pathogenesis of the Crouzon craniostenotic defects. *Cleft Palate J.* 1986;23:28–39.
33. Persing JA, Jane JA. Treatment of syndromic and nonsyndromic bilateral coronal synostosis in infancy and childhood. *Neurosurg Clin N Am.* 1991;2:655–663.
34. Hoyte DA. The cranial base in normal and abnormal skull growth. *Neurosurg Clin N Am.* 1991;2:515–537.
35. Burrows AM, Richtsmeier JT, Mooney MP, et al. Three-dimensional analysis of craniofacial form in a familial rabbit model of nonsyndromic coronal suture synostosis using Euclidean distance matrix analysis. *Cleft Palate Craniofac J.* 1999;36:196–206.
36. Mooney MP, Losken HW, Tschakaloff A, et al. Congenital bilateral coronal suture synostosis in a rabbit and craniofacial growth comparisons with experimental models. *Cleft Palate Craniofac J.* 1993;30:121–128.
37. Carr M, Posnick JC, Pron G, et al. Cranio-orbito-zygomatic measurements from standard CT scans in unoperated Crouzon and Apert infants: comparison with normal controls. *Cleft Palate Craniofac J.* 1992;29:129–136.
38. Forte AJ, Steinbacher DM, Persing JA, et al. Orbital dysmorphology in untreated children with Crouzon and Apert syndromes. *Plast Reconstr Surg.* 2015;136:1054–1062.

39. Tamburrini G, Caldarelli M, Massimi L, et al. Complex craniosynostoses: a review of the prominent clinical features and the related management strategies. *Childs Nerv Syst.* 2012;28: 1511–1523.
40. Dagi LR, MacKinnon S, Zurakowski D, et al. Rectus muscle excyclorotation and V-pattern strabismus: a quantitative appraisal of clinical relevance in syndromic craniosynostosis. *Br J Ophthalmol.* 2017;101:1560–1565.
41. Kreiborg S, Cohen MM Jr. Ocular manifestations of Apert and Crouzon syndromes: qualitative and quantitative findings. *J Craniofac Surg.* 2010;21:1354–1357.
42. Greig AV, Britto JA, Abela C, et al. Correcting the typical Apert face: combining bipartition with monobloc distraction. *Plast Reconstr Surg.* 2013;131:219e–230e.
43. Medicine NUSNLo. *Apert Syndrome.* 2018. Available at https://ghrnlmnihgov/condition/apert-syndrome#statistics.